Study of 375nm ultraviolet InGaN/AlGaN light-emitting diodes with heavily Si-doped GaN transition layer in growth mode, internal quantum efficiency, and device performance

Shih-Cheng Huang, Kun-Ching Shen, Dong-Sing Wuu, Po-Min Tu, Hao-Chung Kuo, Chia-Cheng Tu, and Ray-Hua Horng

Citation: Journal of Applied Physics **110**, 123102 (2011); doi: 10.1063/1.3669377
View online: http://dx.doi.org/10.1063/1.3669377
View Table of Contents: http://scitation.aip.org/content/aip/journal/jap/110/12?ver=pdfcov
Published by the AIP Publishing

Study of 375 nm ultraviolet InGaN/AlGaN light-emitting diodes with heavily Si-doped GaN transition layer in growth mode, internal quantum efficiency, and device performance

Shih-Cheng Huang,[1,6] Kun-Ching Shen,[1] Dong-Sing Wuu,[1,5,a)] Po-Min Tu,[2] Hao-Chung Kuo,[2] Chia-Cheng Tu,[3] and Ray-Hua Horng[4,7]
[1]*Department of Materials Science and Engineering, National Chung Hsing University, Taichung 40227, Taiwan*
[2]*Department of Photonics and Institute of Electro-Optical Engineering, National Chiao-Tung University, Hsinchu 30010, Taiwan*
[3]*Department of Electronic Engineering, Faculty of Engineering, Chung Yuan Christian University, Chungli 32023, Taiwan*
[4]*Institute of Precision Engineering, National Chung Hsing University, Taichung 40227, Taiwan*
[5]*Department of Materials Science and Engineering, Da-Yeh University, Changhua 51591, Taiwan*
[6]*Advanced Optoelectronic Technology Inc., Hsinchu 30352, Taiwan*
[7]*Advanced Optoelectronic Technology Center, National Cheng Kung University, Tainan 701, Taiwan*

(Received 15 June 2011; accepted 14 November 2011; published online 20 December 2011)

High performance 375 nm ultraviolet (UV) InGaN/AlGaN light-emitting diodes (LEDs) were demonstrated with inserting a heavy Si-doped GaN transition layer by metal-organic chemical vapor deposition. From transmission electron microcopy (TEM) image, the dislocation densities were significantly reduced due to the existence of the heavily Si-doping growth mode transition layer (GMTL), which results in residual stress relaxation and 3D growth. The internal quantum efficiency (IQE) of the LEDs with GMTL was measured by power-dependent photoluminescence (PL) to be 40.6% higher than ones without GMTL. The GMTL leads to the superior IQE performance of LEDs not only in decreasing carrier consumption at nonradiative recombination centers but also in partially mitigating the efficiency droop tendency. When the vertical-type LED chips (size: 1 mm × 1 mm) was driven with a 350 mA injection current, the output powers of the LEDs with and without GMTL were measured to be 286.7 and 204.2 mW, respectively. A 40.4% enhancement of light output power was achieved. Therefore, using the GMTL to reduce dislocations would be a promising prospective for InGaN/AlGaN UV-LEDs to achieve high IQE.
 [doi:10.1063/1.3669377]

I. INTRODUCTION

Nitride-based ultraviolet light-emitting diodes (UV-LEDs) have recently attracted great attention due to their promising potential to replace conventional mercury-containing lamps for some lighting applications, including UV sensing, curing, and photocatalysis. UV-LEDs are also used as a pumping source for developing white-light LEDs and to solve the low color-rendering-index problem caused by the combination of a blue LED chip with an yttrium-aluminum-garnet phosphor.[1–3] As a result, enhancing luminescence and efficiency of UV-LEDs becomes more important for these applications. For blue- and green-emitting LEDs, it is well known that high radiative efficiency is mainly attributed to the localized states originating from the phase separation or fluctuations of the indium content in the InGaN/GaN quantum well (QW). However, the indium concentration in the active region of UV-LEDs is much lower than in blue or green LEDs, which leads to less localized states because phase separation do not easily occur at low indium concentration. Besides, low indium content creates a small bandgap discontinuity at the InGaN(well)/GaN(barrier) interface, and decreases the carrier confinement effect. These effects have been shown to cause a low radiative efficiency in UV-LEDs.[4–6] In addition, the threading dislocation (TD) density of the GaN epilayer is as high as 10^9 cm^{-2} because of growth on a lattice-mismatched sapphire substrate. The dislocations generally act as nonradiative recombination centers that degrade the performance of the light emitters. UV-LEDs are particularly sensitive to the dislocation density.[7,8]

Recently, epitaxial lateral overgrowth (ELOG) and patterned sapphire substrate (PSS) have been identified as effective methods to reduce the TD density to 10^7 cm^{-2}.[9–12] However, the ELOG technique usually requires a two-step metal-organic chemical vapor deposition (MOCVD) growth, which decreases the production yield and results in chamber contaminations. On the other hand, the crystal quality of the PSS epilayer strongly depends on the pattern shape, pattern size, and facet angle, parameters that are not easy to control on sapphire. A growth technique employing *in situ* SiN_x as a nanoscale masks has been demonstrated as another choice for reducing TDs.[13,14] The *in situ* SiN_x deposited by modulating ammonia (NH_3) and silane (SiH_4) flow can be directly grown on a nucleation layer or un-doped GaN without interrupting the growth process. While it offers a fast and simple method leading to TDs reduction, the SiN_x shows poor heat dissipation properties and is not desirable for inclusion in LED.

a)Author to whom correspondence should be addressed. Electronic mail: dsw@dragon.nchu.edu.tw. Fax: +886-4-22855046.

Therefore, in this study, we investigate an *in situ* growth mode transiting technique to achieve low TD density and high emission efficiency UV-LEDs. Unlike the *in situ* SiN_x method above, we doped an *n*-GaN layer heavily with Si to create a growth mode transition layer (GMTL). Such a heavily doped layer was expected to release the residual strain through bending dislocations.[15] Meanwhile, to prevent the deposition of SiN_x, a high Si flux was maintained during GMTL growth process. Additionally, AlGaN barrier layers were also used instead of GaN barrier layers to increase the carrier confinement effect in these UV-LEDs. The effects of inserting the GMTL in growth mode on the internal quantum efficiency (IQE) and the device properties of the UV-LEDs were thoroughly investigated by transmission electron microcopy (TEM), scanning electron microscopy (SEM), power- and temperature-dependent photoluminescence (PL), and device performance measurements.

II. EPITAXIAL GROWTH AND DEVICE FABRICATION

All LEDs in this study were grown on 2-in. *c*-plane sapphire substrates using an MOCVD system. Trimethylgallium, trimethylindium, trimethylaluminum, and NH_3 were employed as the reactant source materials. Bicyclopentadienyl magnesium and SiH_4 were used as the *p*-type and *n*-type doping sources, respectively. Prior to the growth, the sapphire substrate was thermally cleaned in hydrogen ambient at 1100 °C. The LED was designed for a 375 nm emission wavelength by depositing a 30 nm low-temperature (500 °C) GaN buffer layer, a 2 μm un-doped GaN layer, a 50 nm heavily Si-doped GaN layer as GMTL, a 2.5 μm *n*-AlGaN contact layer, an MQW active region, a 15 nm Mg-doped AlGaN cladding layer, and a 0.2 μm Mg-doped GaN contact layer. The MQW consists of ten periods of 3 nm $In_{0.03}Ga_{0.97}N$ well layers and 11 nm $Al_{0.06}Ga_{0.94}N$ barrier layers. The Si-doping concentration of the *n*-AlGaN layer and GMTL are 4.5×10^{18} and $1.2 \times 10^{20}\,cm^{-3}$ controlled by different SiH_4 flow rates. A UV-LED without GMTL was fabricated as a control sample.

The TD distribution was observed by TEM images. To realize the growth mode transition, surface morphologies of the *n*-AlGaN layer grown on the GMTL with different overgrowth times were examined by SEM. Power- and temperature-dependent PL measurements were carried out using a frequency-tripled Ti:sapphire laser with a wavelength of 266 nm. The details of the excitation laser system and PL measurement can be found in Ref. 16. Finally, the LED wafers were processed into vertical type chips (size: 1 mm × 1 mm), and LED chips with and without GMTL were denoted as G-LEDs and C-LEDs, respectively. The light output-current (L-I) and current-voltage (I-V) characteristics of the LED devices were measured using an integrating sphere detector and Keithley 2400 at room temperature.

III. RESULTS AND DISCUSSION

Fig. 1 shows a schematic of the UV-LED structure. The inset of Fig. 1 shows a TEM image of the GMTL region. It is clear that some TDs have bent or stopped propagating into the *n*-AlGaN layer due to the existence of the GMTL. The TDs behavior was partially attributed to the relaxation of residual stresses in the un-doped GaN by Si incorporation,[15] especially for GMTL with $10^{20}\,cm^{-3}$ Si concentrations. However, compared with Ref. 15, our GMTL thickness is too thin to fully release residual stress, which induces a three-dimensional (3D) growth. The 3D growth may be another possible cause of TDs bending or stopping. Based on the observation above, the TDs were effectively reduced by the inclusion of the GMTL.

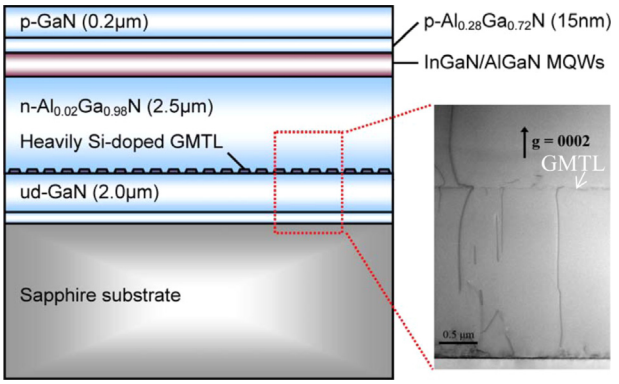

FIG. 1. (Color online) Schematic structure of UV-LEDs. The inset shows the TEM images within GMTL.

The evolution of growth mode transition on the GMTL with different overgrowth times is shown in Fig. 2. In Fig. 2(a), one can see that the as-grown GMTL is associated with GaN islands with dimensions of 100-200 nm. This indicates that the GaN growth mode has made a transition from layer-by-layer growth (2D growth) to 3D growth. The high

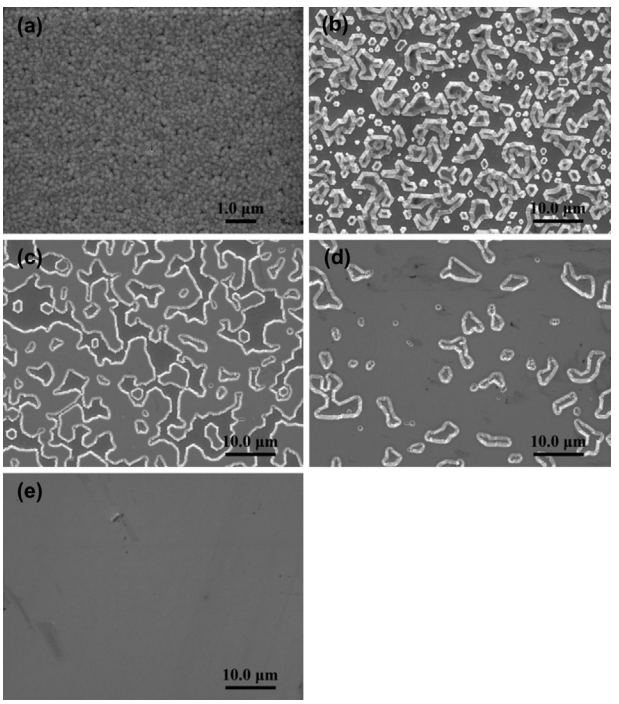

FIG. 2. SEM micrographs of the (a) as-grown GMTL and *n*-AlGaN layer with different overgrowth times (b) 10, (c) 20, (d) 30, (e) 60 min, respectively.

Si concentration changes the surface energy of un-doped GaN during the growth process, influencing the GaN growth mode and results in GaN island growth.[17] In Figs. 2(b)–2(d), when increasing the AlGaN overgrowth time from 10, 20 to 30 min, the AlGaN islands grow on GaN islands and start to meet through lateral growth, similar to ELOG. After 60 min overgrowth time, full coalescence generates a smooth surface (Fig. 2(e)). Both TEM and SEM results confirm the effects of heavy Si-doping in TD reduction are residual stress release and 3D growth. While the GMTL thickness is insufficient to fully release stress, the TDs are reduced by lateral growth process on GaN islands. Moreover, the TD densities of AlGaN with and without GMTL were evaluated by an etch-pit-density (EPD) measurement with KOH solution, as shown Fig. 3. The TD value of AlGaN grown on GMTL was significantly decreased from the control sample value of 8×10^8 to $8 \times 10^7\,cm^{-2}$. Meanwhile, the full-width at half-maximum (FWHM) of (002) and (102) x-ray diffraction peaks was measured by double crystal x-ray diffraction (DC-XRD). On comparison with the AlGaN without GMTL, the FWHM of AlGaN with GMTL for the (002) plane dropped from 360 to 270 arc sec. Similarly, for the (102) plane, the FWHM value became from 460 to 380 arc sec. From the XRD results, the AlGaN with GMTL exhibits better crystal quality than that without GMTL because the GMTL structure suppresses the TD extensions.

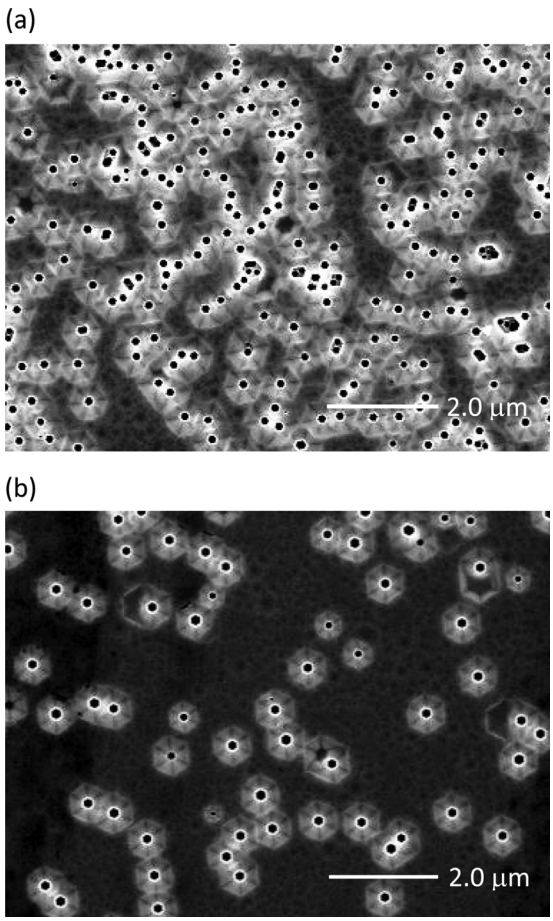

FIG. 3. Typical plane-view SEM micrographs of etch pit density with KOH etched *n*-AlGaN surface (a) without GMTL, (b) with GMTL.

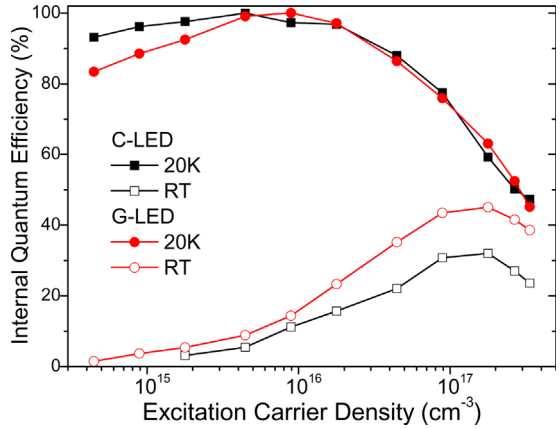

FIG. 4. (Color online) Internal quantum efficiency of LEDs at 20 K and RT as a function of excitation carrier density.

As described above, lower TD density UV-LEDs were obtained by including a GMTL; the reduction of these nonradiative recombination centers implies that the IQE of LEDs can be improved through this growth process. Generally, the ratio of the integrated PL intensities measured at room-temperature over low-temperature is expressed as the IQE value. This IQE estimation method involves the assumption that PL efficiency at low-temperature is equal to 100%. However, in fact the IQE value is usually underestimated due to the strong dependence of the PL efficiency on the density of nonradiative centers even at low-temperature. It means the IQE value obtained by the traditional method cannot completely reflect the true quantum efficiency. A more accurate IQE determination method through measuring PL spectra with varying excitation carrier density and temperature has been proposed,[16,18] our IQE data is based on this measurement method.

Fig. 4 shows the power-dependent IQE as a function of injected carrier density at 20 K and room-temperature (RT) for both C-LED and G-LED. The IQE is defined as the collected photon numbers divided by the injected photon numbers and normalized to the maximum efficiency achieved at 20 K. For the two LEDs, the IQE curves are very similar at 20 K. At low excitation carrier density ($<10^{16}\,cm^{-3}$), the IQE increase may be attributed to the saturation of nonradiative recombination centers by photo-generated carriers. It seems that the nonradiative centers still influence the efficiency at low-temperature. Moreover, the IQE decreases with a further increase in the excitation carrier density ($>10^{16}\,cm^{-3}$). This phenomenon is quite similar to "efficiency droop," the gradual decrease of the power efficiency of LEDs as the injection current increases. Although several mechanisms for explaining the efficiency droop have been reported, including carrier leakage and carrier overflow,[19–21] direct or indirect Auger recombination,[22,23] defects (or dislocations),[24,25] and the delocalization from InN fluctuations,[26] the main mechanism in the efficiency droop still remains unclear. According to our experimental data, we infer that the low-temperature IQE decrease at high excitation carrier density is due to the carrier overflow and dislocation density, which is further discussed in Fig. 5. As the temperature increases to RT, the significant IQE

reduction was attributed to nonradiative recombination at defects and dislocations. In addition, the rise rate of the IQE with increasing excitation carrier density in G-LED is faster than in C-LED. This is because the influence of nonradiative recombination was greatly diminished by reducing the TDs using GMTL. The IQE of G-LED was enhanced by 40.6% compared to that of C-LED. Furthermore, it was observed the IQE droop degree in G-LED at RT is relatively slow in C-LED. It may allow us to attribute the effect of TDs in efficiency droop: at low-temperature, the contribution of dislocations to the IQE droop is weak, and another factor such as carrier overflow is dominant at high excitation carrier density; at room-temperature, the droop efficiency involved with the dislocation contribution leads to a more severe droop trend, which can be suppressed by using low dislocations G-LED.

Fig. 5 shows the PL spectra of G-LED at 20 K under three different excitation carrier densities. At an excitation carrier density over $10^{16}\,cm^{-3}$, a shoulder peak at 380 nm appears in the spectrum and the intensity proportion of the shoulder peak over the main peak gradually increases as excitation carrier increases. The shoulder peak was attributed to the electron overflow into *p*-AlGaN at high carrier density.[27] Likewise, increased carrier density, which reveals the 380 nm peak, corresponds to the onset of efficiency droop (Fig. 4). It indicates that the carriers generated by high excitation exceed the recombination ability in the QW and overflow to *p*-AlGaN layer, emitting 380 nm wavelength photons. Moreover, in contrast with RT, there is no extra peak in PL spectra of G-LED even at high excitation intensity, as shown in the inset of Fig. 5. A similar PL spectrum also occurs in C-LED at 20 K and RT. To summarize, the GMTL leads to the superior IQE performance of G-LED not only by decreasing carrier consumption at nonradiative recombination centers but also by partially mitigating the efficiency droop tendency.

Fig. 6 illustrates the I-V characteristics of both UV-LEDs. With an injection current of 350 mA, the forward voltages were almost the same for both UV-LEDs. However, for the reverse-bias case with a reverse voltage of 5.0 V, the reverse currents were 0.005 and 0.048 μA for G-LED and C-LED, respectively. The inset of Fig. 6 shows the reverse-bias

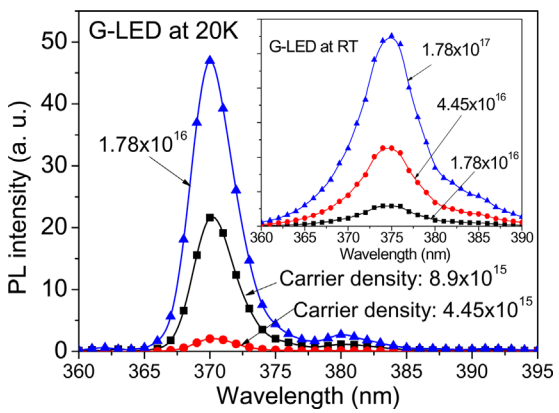

FIG. 5. (Color online) PL spectra of G-LED with three different excitation carrier densities at 20 K. In the inset, PL spectra of G-LED with three different excitation carrier densities at RT.

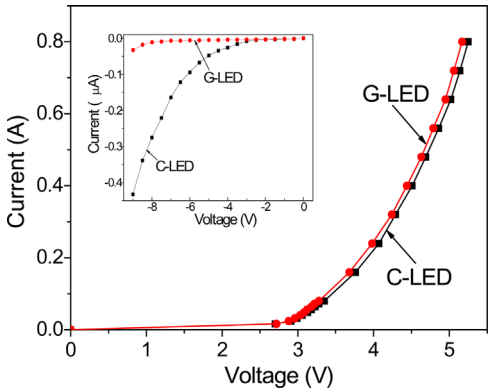

FIG. 6. (Color online) Forward-bias I-V characteristics of the C-LEDs and G-LEDs. The inset shows the reverse-bias I-V characteristics of the C-LEDs and G-LEDs.

I-V characteristics of the C-LED and G-LED. This significant improvement is suggested to be originated from the suppression of leakage current due to the reduction of TDs as discussed above.

Fig. 7 presents the electroluminescence light output power as a function of injection current for both of C-LED and G-LED. Here all chips were Au-wire bonded and packaged using the epoxy-free metal can (TO-66). Clearly, the light output power of the G-LED is much higher than the C-LED over the injection current range of 0 to 1000 mA. When the vertical-type LED chips was driven with a 350 mA injection current, the output power of the LEDs with and without GMTL were measured to be 286.7 and 204.2 mW, respectively. In particular, the light output power of G-LED is enhanced by a factor of approximately 40.4% at an injection current of 350 mA. The inset in Fig. 7 shows the photograph of the vertical-type G-LEDs chip lighting on.

IV. CONCLUSION

High-quality UV-LEDs were successfully fabricated using an MOCVD system by inserting GMTL between undoped GaN and *n*-AlGaN. Cross-sectional TEM observations revealed that the TDs in the *n*-AlGaN layer were effectively reduced through residual stress relaxation and 3D growth. As a result, the reverse-bias current of the LED with GMTL was much smaller than that of the LED without GMTL.

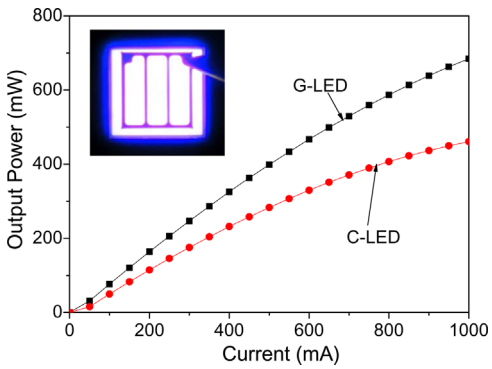

FIG. 7. (Color online) LED output power as functions of injection current of G-LED and C-LED. In the inset, photograph of the G-LEDs chip lighting on at 350 mA.

Meanwhile, the relative light output power was found to be enhanced by a factor of approximately 40.4% at an injection current of 350 mA. These results suggest that the use of the GMTL is effective at elevating the quality of GaN-based UV emitters.

ACKNOWLEDGMENTS

This research was supported by National Science Council (Taiwan) under Contract No. 98-2221-E-005-005-MY3 and 98-3114-E-005-002-CC2.

[1]C. H. Kuo, J. K. Sheu, S. J. Chang, Y. K. Su, L. W. Wu, J. M. Tsai, C. H. Liu, and R. K. Wu, Jpn. J. Appl. Phys. **41**, L1434 (2002).
[2]H. Hirayama, T. Yatable, N. Noguxhi, T. Ohashi, and N. Kamata, Appl. Phys. Lett. **91**, 071901 (2007).
[3]Y. S. Tang, S. F. Hu, C. C. Lin, N. C. Bagkar, and R. S. Liu, Appl. Phys. Lett. **90**, 151108 (2007).
[4]S. F. Chichibua, T. Azuhata, T. Sota, and S. Nakamura, Appl. Phys. Lett. **69**, 4188 (1996).
[5]S. J. Chang, C. H. Kuo, Y. K. Su, L. W. Wu, J. K. Sheu, T. C. Wen, W. C. Lai, J. F. Chen, and J. M. Tsai, IEEE J. Sel. Top. Quantum Electron. **8**, 744 (2002).
[6]I. H. Ho, Appl. Phys. Lett. **69**, 2701 (1996).
[7]S. D. Lester, F. A. Ponce, M. G. Craford, and D. A. Steigerwald, Appl. Phys. Lett. **66**, 1249 (1995).
[8]T. Wang, Y. H. Liu, Y. B. Lee, Y. Izumi, J. P. Ao, J. Bai, H. D. Li, S Sakai, J. Cryst. Growth **235**, 177 (2002).
[9]J. H. Cheng, Y. C. S. Wu, W. C. Liao, and B. W. Lin, Appl. Phys. Lett. **96**, 051109 (2010).
[10]H. W. Huang, J. K. Huang, S. Y. Kuo, K. Y. Lee, and H. C. Kuo, Appl. Phys. Lett. **96**, 263115 (2010).
[11]D. S. Wu, W. K. Wang, K. S. Wen, S. C. Huang, S. H. Lin, S. Y. Huang, C. F. Lin, and R. H. Horng, Appl. Phys. Lett. **89**, 161105 (2006).
[12]Y. Li, S. You, M. Zhu, L. Zhao, W. Hou, T. Detchprohm, Y. Taniguchi, N. Tamura, S. Tanaka, and C. Wetzel, Appl. Phys. Lett. **98**, 151102 (2011).
[13]X. L. Fang, Y. Q. Wang, H. Meidia, and S. Mahajan, Appl. Phys. Lett. **84**, 484 (2004).
[14]J. Hertkorn, F. Lipski, P. Bruckner, T. Wunderer, S. B. Thapa, F. Scholz, A. Chuvilin, U. Kaiser, M. Beer, and J. Zweck, J. Cryst. Growth **310**, 4867 (2008).
[15]I. H. Lee, I. H. Choi, C. R. Lee, and S. K. Noh, Appl. Phys. Lett. **71**, 1359 (1997).
[16]Y. J. Lee, C. H. Chiu, C. C. Ke, P. C. Lin, T. C. Lu, H. C. Kuo, and S. C. Wang, IEEE J. Sel. Top. Quantum Electron. **15**, 1137 (2009).
[17]H. Lahreche, P. Vennegues, B. Beaumont, and P. Gibart, J. Cryst. Growth **205**, 245 (1999).
[18]S. Watanabe, N. Yamada, M. Nagashima, Y. Ueki, C. Sasaki, Y. Yamada, T. Taguchi, K. Tadatomo, H. Okagawa, and H. Kudo, Appl. Phys. Lett. **83**, 4906 (2003).
[19]I. A. Pope, P. M. Smowton, P. Blood, J. D. Thomson, M. J. Kappers, and C. J. Humphreys, Appl. Phys. Lett. **82**, 2756 (2003).
[20]K. J. Vampola, M. Iza, S. Keller, S. P. DenBaars, and S. Nakamura, Appl. Phys. Lett. **94**, 061116 (2009).
[21]C. H. Wang, C. C. Ke, C. Y. Lee, S. P. Chang, W. T. Chang, J. C. Li, Z. Y. Li, H. C. Yang, H. C. Kuo, T. C. Lu, and S. C. Wang, Appl. Phys. Lett. **97**, 261103 (2010).
[22]Y. C. Shen, G. O. Mueller, S. Watanabe, N. F. Gardner, A. Munkholm, and M. R. Krames, Appl. Phys. Lett. **91**, 141101 (2007).
[23]E. Kioupakis, P. Rinke, K. T. Delaney, and C. G. Van de Walle, Appl. Phys. Lett. **98**, 161107 (2011).
[24]N. I. Bochkareva, V. V. Voronenkov, R. I. Gorbunov, A. S. Zubrilov, Y. S. Lelikov, P. E. Latyshev, Y. T. Rebane, A. I. Tsyuk, and Y. G. Shreter, Appl. Phys. Lett. **96**, 133502 (2010).
[25]M. F. Schubert, S. Chhajed, J. K. Kim, E. F. Schubert, D. D. Koleske, M. H. Crawford, S. R. Lee, A. J. Fischer, G. Thaler, and M. A. Banas, Appl. Phys. Lett. **91**, 231114 (2007).
[26]J. Wang, L. Wang, W. Zhao, Z. Hao, and Y. Luo, Appl. Phys. Lett. **97**, 201112 (2010).
[27]A. Chitnis, J. P. Zhang, V. Adivarahan, M. Shatalov, S. Wu, R. Pachipulusu, V. Mandavilli, and M. Asif Khan, Appl. Phys. Lett. **82**, 2566 (2003).